Inorganic Chemistry

ARTICLE

pubs.acs.org/IC

Assessment of the Electronic Structure of 2,2′-Pyridylpyrrolides as Ligands

Jaime A. Flores,[†] José G. Andino,[†] Nikolay P. Tsvetkov,[†] Maren Pink,[†] Robert J. Wolfe,[†] Ashley R. Head,[‡] Dennis L. Lichtenberger,[‡] Joseph Massa,[†] and Kenneth G. Caulton*[,†]

[†]Department of Chemistry, Indiana University, Bloomington, Indiana 47405, United States

[‡]Department of Chemistry and Biochemistry, The University of Arizona, Tucson, Arizona 85721, United States

Supporting Information

ABSTRACT: The ligand class 2,2′-pyridylpyrrolide is surveyed, both for its structural features and its electronic structure, when attached to monovalent K, Cu, Ag, Au, and Rh. The influence of pyrrolide ring substituents is studied, as well as the question of push/pull interaction between the pyridyl and pyrrolide halves. The π donor ability of the pyrrolide is found to be less than that of an analogous phenyl. However, in contrast to the phenyl analog, the HOMO is pyrrolide π in character for pyridylpyrrolide complexes of copper and rhodium, while it is conventionally metal localized for planar, d^8 rhodium pyridylphenyl. Monovalent three-coordinate copper complexes show great deviations from Y-shaped toward T-shaped structures, including cases where the pyridyl ligand bonds only weakly.

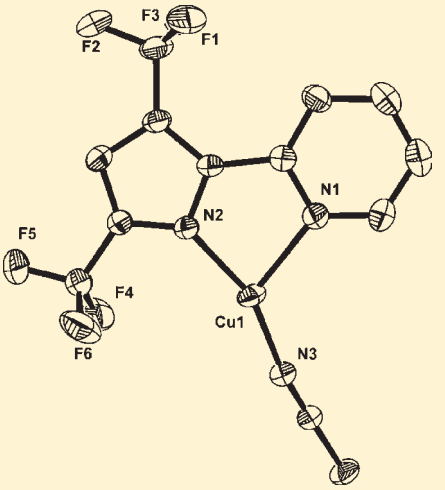

INTRODUCTION

We are interested in a ligand type which combines amide character with modular steric modification. The pyridyl pyrrolides $(L^n)^{-1}$ appear to offer this possibility (Scheme 1) since their synthesis[1] involves ring closure of a β diketone (residue in red in Scheme 1) with an aminomethylpyridine. Because of the synthetic method and the ready availability of β diketonates, including those with two different substituents, a wide range of pyridylpyrroles become available, to allow testing, in metal complexes, of the influence on reactivity of electron donating and withdrawing groups and also of differing steric effects. Ligands **1**−**3** (Scheme 1) show a few of the ligands investigated recently,[2−19] primarily as ancillaries for olefin polymerization catalysts. Some of these include two imines, while others have an imine and a pyrrolide, but none of these combine the anion character with the possibility of delocalization through two rings found in pyridylpyrrolides. Azolate complexes, with two or more nitrogens in a five-membered ring, are actively studied for their photophysical properties and as olefin polymerization ancillaries.[20−22] However, the many nitrogens reduce ring nucleophilicity compared to that of a pyrrolide.

We seek to exploit the 2-pyridylpyrrolide class of ligands as possibly redox active and thus useful auxiliaries to expand the redox activity of their metal complexes beyond simply metal-centered oxidation. While pyridylpyrrolide ligands have seen considerable recent research activity,[23−29] they have not been considered redox active. Our goal in the present article is to evaluate the general characteristics of pyridylpyrrolides, both structural and electronic, in anticipation of exploring the redox behavior of their metal complexes.

What is the degree of π donation from the pyrrole to a metal, and how is this influenced by the *constraints* of it being in a chelate with pyridine as the second donor? For comparison, Hammett studies of metal-free pyrroles have shown that they are π donors when attached to phenyl via N or any pyrrole ring carbon.[30−32] As a substituent on an aryl (pyridine) ring, pyrrolide thus gives amide character to the pyridine partner **4**, provided there is conjugation between the two rings.

4: 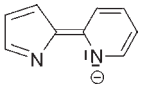

For oxidative applications, it is especially appropriate to use N/N ligands at the imine oxidation level, since, unlike amines,

Received: March 17, 2011
Published: July 21, 2011

   dx.doi.org/10.1021/ic2005503 | *Inorg. Chem.* 2011, 50, 8121–8131

Scheme 1

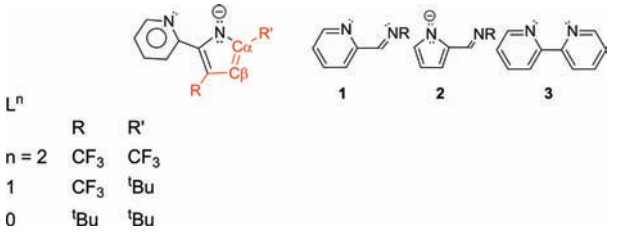

these cannot be dehydrogenated (i.e., oxidized), and certainly imine nitrogen (vs amine N) itself resists further oxidation. By contrast, iminocatecholate ligands have been shown to undergo attack by O_2.[33]

It is worth noting that this ligand type differs from the many redox active ligands that are currently being studied[34−42] since those are generally 2-fold symmetric, with two identical donors (monoiminocatecholates, while not C_2 symmetric, nevertheless involve analogous donors). In other words, pyridylpyrrolides attached to a redox active metal offer pyridine π^* orbitals as an electron acceptor and pyrrolide occupied π orbitals as a donor, when a pyridylpyrrolide/metal complex is reduced or oxidized, respectively. They thus potentially represent a push/pull pair, not only to each other (**4**) but also toward the redox chemistry of an attached metal. This will influence the redox potential of the combined bidentate metal/ligand system.

All of the above can be modulated by substituents on the pyrrole ring, and so we will investigate both electron-withdrawing CF_3 and electron-donating ^{t}Bu substituents. While pyrroles are well-known for being oxidizable, the rapid follow-up coupling of their radical cations to form oligo- and polypyrroles will perhaps be less likely if the radical cation is bound to a metal center. Finally, we are interested in evaluating the expectation that a CF_3 substituent on C_α of the pyrrole can resist attack by a highly electrophilic metal center so that the electrophilicity can be retained at the metal center and be focused on bimolecular reactivity. For comparison, it is known that a ^{t}Bu substituent at Cα can be attacked by a metal center.[26] Throughout this work, the fact that the pyrrole nitrogen π lone pair is to some extent "committed" to the aromaticity of pyrrole is modulated by the fact that the resonance energy of pyrrole is less than that of benzene by ∼30% or 10−15 kcal/mol.[43]

The substituent pattern on these pyrrole rings is also optimal for preventing the intrinsic reactivity of pyrroles under oxidizing conditions: oxidative coupling (eq 1) at the ring carbons,[19] creating dimers, and even polymers (polypyrroles). Three of the pyrrole ring carbons in the L^n studied here are protected by substitution, and the fourth one is sterically protected.

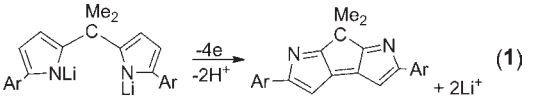

(1)

We present here an evaluation of these monoanionic ligands from the perspective of experimental studies, both spectroscopic and structural, and also DFT computational evaluation of their orbital composition and energies. We recently reported the chemistry of L^2 with monovalent copper,[44] which we will evaluate here in further detail on the basis of our general analysis of the ligands, which we now report.

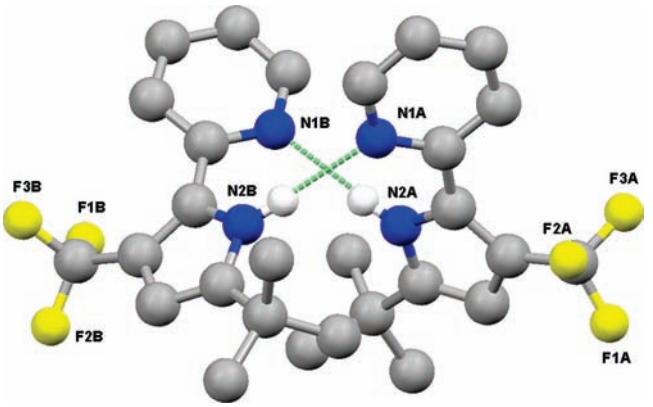

Figure 1. Mercury view of the structure of HL^1 with hydrogens omitted for clarity. Unlabeled atoms are carbons. The NH hydrogens are shown.

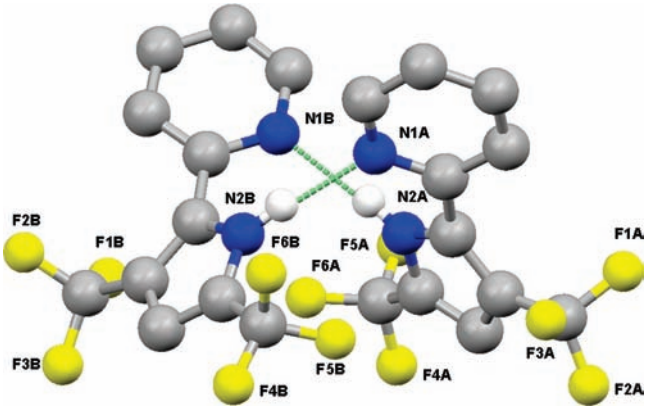

Figure 2. Mercury view of the structure of HL^2 with hydrogens on carbon omitted for clarity. Unlabeled atoms are carbons.

RESULTS

We study three examples spanning a range of electron-withdrawing (CF_3) and -donating groups (tBu). These are abbreviated with a designator *n* (Scheme 1), which is the number of CF_3 groups. The spectroscopic properties of these three HL^n's are conventional. Proton NMR of the L ligands in diamagnetic compounds shows a sharp singlet for the proton on the pyrrole ring carbon. Of the four chemical shifts for the pyridyl ring hydrogens, the most positive chemical shift is routinely assigned to the H ortho to the nitrogen (this is typical for all pyridines), and the H nearest the ring junction is also a doublet. The other two hydrogens are apparent triplets. We have determined the single crystal structures of HL^2 and HL^1 (Figures 1 and 2); as found earlier[29,45] for other substituent examples, these exist as dimers held together by head to tail hydrogen bonds. These would have an unfavorable, highly bent N−H···N angle if hydrogen bonding were intramolecular. Our structure of material with identical spectra to those reported[29] for HL^1 revealed that 2D NOESY determination of the tBu location was erroneous, and the tBu group is actually located on Cα, adjacent to nitrogen. The two solids in Figures 1 and 2 are not crystallographically isomorphous, but the molecules themselves are essentially isostructural, with only modest dimensional differences.

dx.doi.org/10.1021/ic2005503 |*Inorg. Chem.* 2011, 50, 8121–8131

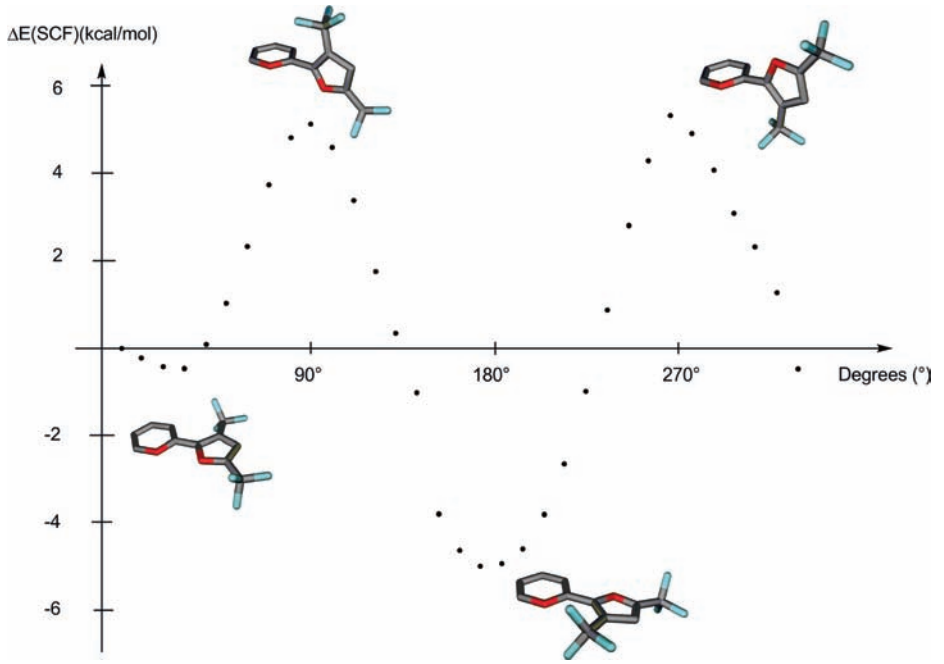

Figure 3. DFT energy of the anion $(L^2)^{-1}$ as a function of the angle of rotation between the two rings. Nitrogens are shown in red.

Hydrogen bonds for HL^2 show a N/N distance of 2.923(3) and 2.879(3) Å and have an NHN angle of >172°. Dihedral angles between the two rings in a given L^2 are 32.1(3) and 36.7(3)°. Hydrogen bonds for HL^1 showed a N/N distance of 3.012(2) and 3.037(2) A and have an NHN angle of >175°; hence, there are longer hydrogen bonds for the less acidic amine. Dihedral angles between the two rings of a given L^1 are 33.5(3)° and 32.7(3)°.

Since this dimerization necessitates twisting of the two rings in one HL^n ~ 33° away from being coplanar, we were interested in the energy cost of such a rotation. Conjugation between the two rings in one HL^n will of course resist the twisting, and the barrier to rotation will then be some gauge of the degree of push/pull conjugation between the pyridyl and pyrrolide rings. For this purpose, we chose to study computationally (DFT, B3LYP) here the anion, to avoid biasing the results from any intramolecular hydrogen bonding of pyrrole NH to the pyridyl nitrogen.

As shown in the rotational profile in Figure 3, $(L^2)^{-1}$ is indeed least stable when the two rings are orthogonal, is 9 kcal/mol more stable when the two nitrogens are *anti*, and is less stable when the nitrogens are *syn* (due to repulsion between the nitrogen lone pairs). The resulting hydrogen bond strength in HL^n must thus exceed this, in addition to exceeding the room temperature $T\Delta S$ value for dimerization of approximately 11 kcal/mol.

HL^n Redox Capacity in the Gas Phase. In order to obtain an experimental measure of the perturbation of the tBu and CF_3 substitutions on the electronic energies of these molecules, gas-phase UV photoelectron spectra were collected for all three HL^n molecules and are provided in the Supporting Information. These spectra show a first ionization band that is well-separated from groupings of less-separated ionizations at higher energies. The valence ionizations expected in this region derive from those of pyrrole[46,47] (which has a π ionization at 8.2 eV well-separated from a second π ionization at 9.2 eV) and the spectrum of pyridine[48] (which has the nitrogen σ lone pair ionization at 9.6 eV and the π ionizations at 9.75 and 10.5 eV). This order for the ionizations of the HL^n molecules is supported by the calculations, which indicate that the lowest energy ionization corresponds to removal of an electron from the π orbital of the pyrrolyl portion of the molecule having a node at the pyrrolyl nitrogen atom (*vide infra*, Figure 8) and somewhat delocalized with the corresponding π orbital of the pyridyl portion of the molecule (see orbital plots in the Supporting Information). The second ionization corresponds to the second π orbital of pyrrolyl with nodes near the 2 and 5 carbon atoms and entirely localized on the pyrrolyl. The third ionization is predominantly from the nitrogen lone pair of the pyridyl portion of the molecule.

Interestingly, the ionization energies of all three orbitals are shifted substantially with the substitution of CF_3 groups for tBu groups (see Supporting Information). The pyridyl nitrogen lone pair ionization is the most relevant to the interaction with the metal frontier orbitals because in the deprotonated, anionic form of the ligands, this orbital mixes with the pyrrolide nitrogen lone pair to form the chelate ligand orbitals that σ-bond to the metal. The ionization energy of the pyridyl N lone pair increases by 0.47 eV from HL^0 to HL^1. Replacing all of the tBu groups with CF_3 groups increases the ionization energy by another 0.56 eV. The nitrogen lone pair ionizations of substituted pyridines have been correlated with the pK_a values and solution phase substituent constants.[48] In the case of substituted pyridines, the nitrogen lone pair ionizations shift in the same directions with alkyl and fluoro substituents on pyridine as with the tBu and CF_3 substituents on these HL^n molecules. For example, adding a tBu group to the 4 position of pyridine lowers the lone pair ionization energy by 0.30 eV,[49] and 2-fluoro-substitution increases the ionization energy by 0.77 eV.[48] The substituent set we employ here thus moves the redox potential of the pyridylpyrrolides a considerable amount.

Pyrrole Deprotonation. Pyrrole deprotonation of HL^2 with KH proceeds smoothly at 25 °C, and the product can be recrystallized from Et_2O with surprising results: it is not simply monomeric KL^2. While the ^{1}H NMR spectrum is unexceptional, a single crystal X-ray structure determination (Figure 4) shows the solid to have formula $KL^2(OEt_2)$ and to adopt a polymeric structure

dx.doi.org/10.1021/ic2005503 |*Inorg. Chem.* 2011, 50, 8121–8131

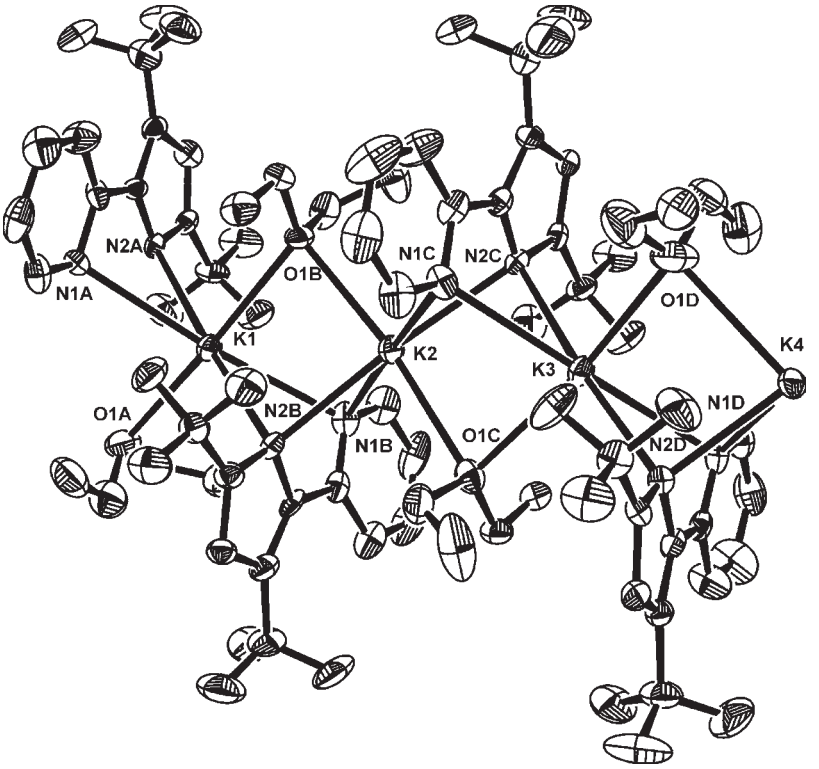

Figure 4. ORTEP view (50% probabilities) of the asymmetric unit of $KL^2(OEt_2)$ polymer, with hydrogens omitted for clarity. Unlabeled atoms are carbons or terminal fluorines.

(Figure 4 and 5) with that as the repeat unit, with four such building blocks in the asymmetric unit. In spite of this, each formula unit has essentially the same structure. The distances between K^+ ions are very symmetric, ranging from 3.888(3) to 3.934(3) Å.

5:

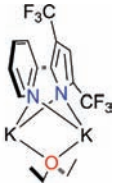

The planar L^2 units are aligned parallel but alternatively up and down in the polymer chain and alternatively down and up are the Et_2O units, which adopt an unusual bridging form between two adjacent K^+ ions. The angles between any three adjacent $K^{+'s}$ all exceed 175°. Since the L^2 anions bridge K^+ ions, *every* nitrogen (pyrrolide and also pyridine) interacts with two K^+; the latter is an unusual structure for a neutral pyridine donor. The dihedral angles N−C−C−N, indicating deviation from planarity of the two rings in a given chelate, are all less than 11.3(7)°. The K/N(pyrrolide) distances range from 2.772(5) to 2.841(5) Å, while those to pyridine are longer at 2.933(5) to 3.010(5) Å. The K^+/O(ether) interaction is evidently "softer" since these distances vary from 2.820(5) to 2.968(4) Å. In summary, every K^+ interacts with four nitrogens and two ether oxygens, with nearly a center of symmetry. The shortest K^+ to ring carbon distances are 3.418(6) Å for pyrrolide and 3.505(6) Å for pyridyl; these always involve the two carbons linking the two nitrogens and are concluded not to involve significant interaction to K^+.

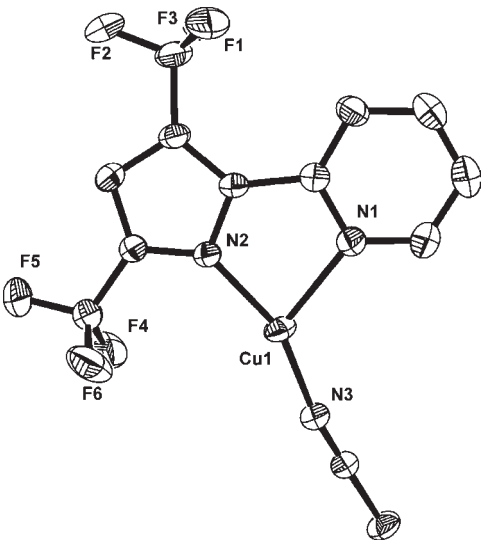

Figure 5. ORTEP view (50% probabilities) of the structure of L^2Cu(NCMe) with hydrogens omitted for clarity. Unlabeled atoms are carbons. Selected structural parameters: Cu1−N3, 1.8437(19) Å; Cu1−N2, 1.9369(17); Cu1−N1, 2.1036(18); N3−Cu1−N2, 157.27(8)°; N3−Cu1−N1, 121.13(8); N2−Cu1−N1, 81.31(7).

The fact that this solid contains four formula units in the asymmetric unit furnishes an especially accurate set of bond lengths for the ligand at this oxidation level. These are summarized in Scheme 2, where the numbers are the average of four determinations, and all have esd's < 0.009 Å. These show that the C/N distance is uniformly shorter than intraring C/C distances, due to the smaller single bond covalent radius of N(sp^2) than C(sp^2).

dx.doi.org/10.1021/ic2005503 |*Inorg. Chem.* 2011, 50, 8121–8131

Scheme 2

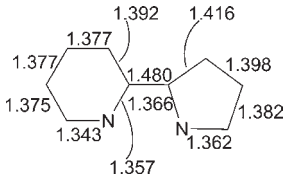

The most distinct value is the C/C distance between the rings, which is longest due to minimal resonance forms with a double bond there. These distances may be used in the future to detect redox chemistry at the ligand.

Cu(I). This synthesis was envisioned as a reaction between a weak acid and a basic metal oxide. Ligand L^2 can be installed on monovalent copper by the reaction of Cu_2O with HL^2 in acetonitrile. For HL^2, the reaction is complete within less than 1 h at 25 °C and is signaled, monitoring NMR spectra during the reaction, by a change of all ^1H and ^{19}F NMR signals of free HL^2 to those of the product, together with a loss of the HL^2 NH proton and growth of a singlet due to liberated water. Product $L^2Cu(NCMe)$ can be isolated by gentle concentration and then cooling and shows a ^1H NMR signal integrating for one MeCN ligand. In the presence of excess MeCN, only one coalesced ^1H NMR signal is seen for free and coordinated MeCN, indicating rapid exchange on the NMR time scale.

The structure of $L^2Cu(NCMe)$ in the solid state (Figure 5) is rigorously planar, including coplanarity of the two rings of the pyridylpyrrolide. There is slight misdirection of the pyridyl and pyrrolide nitrogen lone pairs due to the chelate constraints. The most noteworthy feature of the structure is that the three N−Cu−N angles vary so greatly,[50] with the slender nitrile ligand nevertheless strongly distorted from having equal angles to the chelate nitrogens. This has the effect of putting the nitrile transoid to the pyrrolide nitrogen (angle 157.27(8)°). There is no evidence that this originates from steric repulsion between the nitrile and the CF_3 group; likewise there are no short solid state Cu/F contacts (>3.4 Å). While it is often the case that a ligand trans to an empty coordination site (here pyridyl) bonds *more* strongly, in the present case, the pyridyl nitrogen is 0.16 Å *farther* from copper than the pyrrolide N. The necessary conclusion is that the coordination sphere is "2 + 1," where the latter number designates a distinctly weaker bond. The coordination geometry thus might also be described as T-shaped. The angular differentiation seen in these structures strongly supports the idea that the pyrrolide and pyridyl ligands are electronically very different donors.

In solid $L^2Cu(NCMe)$, the next shortest distance to copper is to N3 of a neighboring molecule, at 3.16 Å. The idea that intermolecular interaction is the cause of the distorted coordination sphere is not attractive since this contact is perpendicular to the coordination plane, hence not on the path toward a tetrahedral structure (note also that Cu, N1, N2, and N3 are coplanar). In addition, since this distortion in the angles to coordinated MeCN is also found in the DFT structure of this species (see below), where neighboring molecules are absent, we conclude that the distortion originates from intramolecular effects, and then this simply lets neighboring molecules approach in the open region of the T-shaped structure.

It is possible to do the synthesis with HL^2 even in nonpolar benzene if the ligand is provided to "stabilize" the otherwise 2-coordinate product. Thus, HL^2 reacts with Cu_2O in benzene within 6 h at 25 °C under 1 atm of CO to give $L^2Cu(CO)$. The CO stretching frequency, 2106 cm^{-1}, shows the presence of only one CO ligand. When HL^n is less Bronsted acidic, thus two ^{t}Bu, HL^0, or one CF_3 and one ^{t}Bu substituents, HL^1, then this Cu_2O-based synthetic reaction fails, even after 48 h at 80 °C.

Table 1. Calculated CO Stretching Frequencies of $L^nM(CO)$

		ν_{CO}, cm^{-1}
		DFT, scaled
$(CF_3)_2$	Cu	2132[a]
$(CF_3)_2$	Ag	2151
$(CF_3)_2$	Au	2128
$(^tBu)_2$	Cu	2109
$(^tBu)_2$	Ag	2125
$(^tBu)_2$	Au	2095

[a] Exptl is 2106.

The binding of CO in $L^2Cu(CO)$ is shown to be completely reversed simply by exposure to a vacuum at 25 °C, and recoordination of CO was proven by subsequent exposure of the CO-free material to CO in a benzene solution. The same reversibility is true for the MeCN adduct. The CO-free material "CuL^2" has been fully characterized as a trimer of unusual connectivity.[44]

The ^{13}C NMR spectrum of $L^2Cu(CO)$ in benzene at 25 °C shows a sharp singlet at 175 ppm. Even in the presence of 1 atm of CO, this chemical shift is unchanged, which indicates that any exchange of free and coordinated CO is slow on the ^{13}C NMR time scale and also that binding of a second CO to $L^2Cu(CO)$ is thermodynamically unfavorable and thus fails to reach detectable population; this last point is in agreement with the low binding energy calculated by DFT (see below). Even under 1 atm of CO at −55 °C in toluene, there is no change in the ^{13}C chemical shift for coordinated CO, indicating that no dicarbonyl is formed.

The situation with $L^2Cu(MeCN)$ is similar: only one methyl ^1H NMR signal is seen for samples of $L^2Cu(NCMe)$ in the presence of increasing amounts of added free MeCN (in the range 1−2 free MeCN per Cu), with the methyl chemical shift moving progressively to higher field. At −60 °C, the two methyl ^1H NMR signals remain coalesced. There is thus no evidence that any $L^2Cu(NCMe)_2$ reaches a detectable population.

Back Donation to CO As a Gauge of Chelate Ligand Donor Power. *a. Cu, Ag, and Au. Structure and Vibrational Frequencies.* In order to evaluate the comparative back bonding abilities of L^nM fragments with a changing principal quantum number, we have carried out a series of comparative DFT(B3LYP) calculations. These have been done first with metals known to be poor π bases, the coinage metals monovalent Cu, Ag, and Au. Considering $L^2M(CO)$ for the comparison series, we find (Table 1 and Figure 6) a trend of ν_{CO} values in the order M = Au < Cu < Ag, and thus apparently the π donor power of the L^2M moiety varies in the opposite direction. This trend is similar to that found experimentally among $[HB(3,5\text{-}(CF_3)_2Pz)_3]M(CO)$ species.[51] The same metal-dependent trend holds for L^1 and L^0 cases, and fewer CF_3 groups lowers the CO frequency, consistent with electron donor trend $L^2 < L^1 < L^0$. Indeed, the silver case here is truly exceptional[52] in that the Ag/C distance[53] is extraordinarily long, at 2.07 Å, fully 0.23 Å longer than it is with copper and 0.15 Å longer than with Au. The structures of all three species are not Y-shaped, which would be characterized by two approximately equal C−M−N angles, but instead T-shaped, with the angle

dx.doi.org/10.1021/ic2005503 |*Inorg. Chem.* 2011, 50, 8121–8131

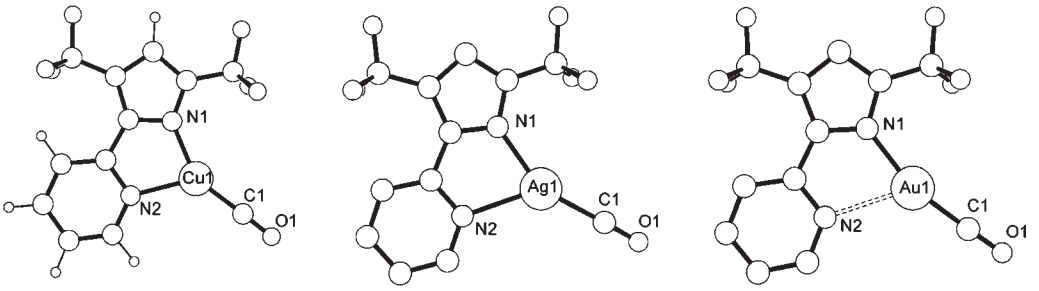

Figure 6. Calculated (DFT) structures of $L^2M(CO)$.

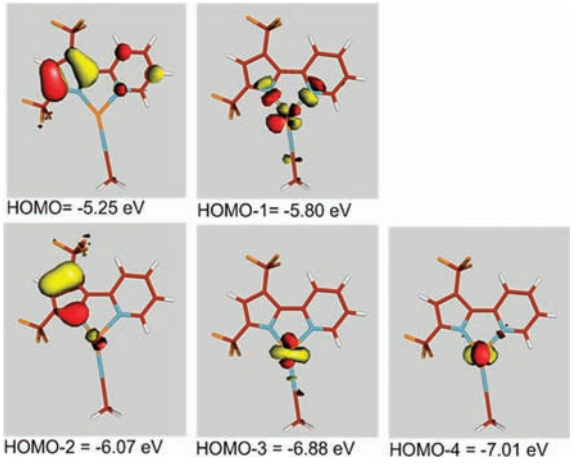

Figure 7. Isodensity contour diagrams of frontier orbitals of L^2Cu-(NCMe).

C−M−N(pyrrolide) being very large, approaching linear. This is what is found experimentally for L^2Cu(NCMe). In fact, the minimum energy structures found show that the pyridyl group bonds more weakly (i.e., longer M/N distances) than the pyrrolide in every case but that the pyridine is exceptionally poorly bonded in the case of gold, where the geometry really tends toward two-coordinate; while pyridine *does* interact with gold, it is certainly very weakly bonded. Thus, the lowest CO stretching frequency for gold is not the result of bonding differences with constant geometry but involves a significant factor of geometry change. Nevertheless, the fact that gold shows the lowest CO stretching frequency is only more surprising in that the lack of a third significant σ donor (pyridine) might be expected to make the gold *less* electron-rich, hence a poorer back bonder; the contrary is observed. Note that this T-shaped structure is like that calculated for MeCN as the third ligand, so change from a poor to a strong π acid ligand does not significantly alter the most stable geometry. Finally, it bears mentioning that all of these ν_{CO} values are extremely high, showing back-donation from these d^{10} species to be very limited.

Orbital Composition. L^2Cu(NCMe) shows an interesting frontier orbital composition. As seen in Figure 7, the frontier orbitals of this neutral, unsaturated species are a mix of ligand-localized (HOMO), pure metal d (HOMO−3 and HOMO−4) and mixed metal/ligand types (HOMO−1 and HOMO−2). HOMO−1 is σ^* (including nitrogens of both pyrrolide and pyridyl), and HOMO−2 is π^* (involving only pyrrolide). None of these have any acetonitrile character. Barring any large geometrical reorganization upon oxidation, L^2Cu(NCMe) should therefore be oxidized at L^2 pyrrolide, but metal d orbitals are nearby and subject to hybridization upon oxidation.

Table 2. Calculated CO Stretching Frequencies of $L''M(CO)_2$

	ν_{CO}, cm^{-1}	
	DFT, scaled	exptl
$(CF_3)_2$/Rh	2102/2042	2086/2016
$(^tBu)_2$/Rh	2077/2023	2066/1995
$(CF_3)_2$/Ir	2087/2027	

Reaction Energies of Monodentate Ligand Binding. The reaction energy for competition between CO and MeCN for the L^2Cu fragment in eq 2 favors coordinated CO by 3.6 kcal/mol.

$$L^2Cu(CO) + MeCN \rightarrow L^2Cu(NCMe) + CO \qquad (2)$$

We interpret this small difference for such electronically different ligands as showing no great preference for the clearly more powerful π acid, CO; hence, it is also evidence for the unimportance of back bonding from d^{10} copper. The reaction energies for binding CO (and MeCN) to two-coordinate L^2Cu are −35.3 (−31.6) kcal/mol. The reaction energies for binding of a *second* CO (or MeCN) to L^2Cu(monodentate) drop to −6.6 (−3.9) kcal/mol. This weak binding energy to form 4-coordinate copper shows that 3-coordinate species are not very "unsaturated," which relates to the observation above that even the third donor, pyridyl, is held at a long distance in an otherwise 2-coordinate, linear copper environment.

b. Rh and Ir. Given the geometry changes, as well as the inherently poor π basicity of the coinage metals, factors which might impede understanding the π donor ability of the $(L^n)M$ fragment, we also calculated $L^nM(CO)_2$, for M = Rh and Ir (Table 2). It was expected that these might have more conventional geometric and electronic structures and thus give simpler trends. Indeed, the complexes are calculated to be conventionally square planar and involve similar distances from metal to pyridyl and pyrrolide nitrogens; the latter are systematically shorter. The lanthanide contraction makes the distances to Ir even slightly shorter than those to Rh. Calculated CO stretching frequencies are consistently lower for Ir than for Rh (in spite of the lanthanide contraction of orbitals acting in the reverse direction). In spite of being dicarbonyls (which should diminish back-donation to a given CO), the stretching frequencies are lower than they are for the coinage metals and thus show greater π donation by the $(L^n)M$ fragment for monovalent Rh and Ir than for Cu, Ag, and Au. The calculated CO vibrational frequency decreases in agreement with ranking ligand donor power as $L^2 < L^0$.

dx.doi.org/10.1021/ic2005503 |*Inorg. Chem.* 2011, 50, 8121–8131

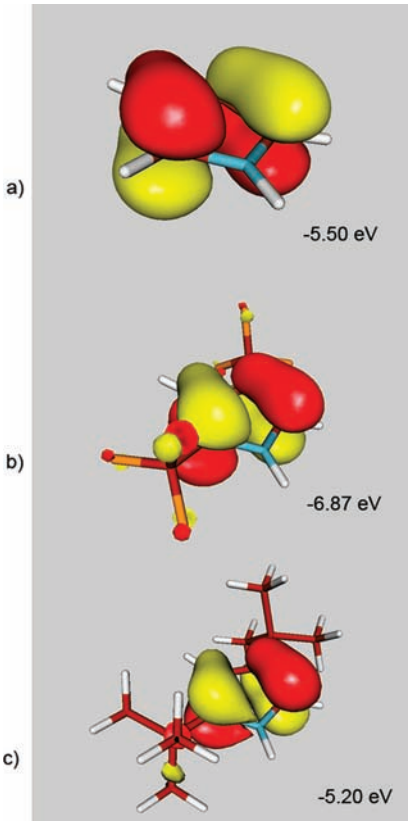

Figure 8. Isodensity plots of the HOMO of (a) pyrrole, (b) 3,5-$(CF_3)_2$ pyrrole, and (c) 3,5-$(^tBu)_2$ pyrrole.

Experimentally, the KL^n reagents described above are synthetically useful. We have reacted KL^n with $[Rh(CO)_2Cl]_n$ in THF and in this way synthesized and characterized two $L^nRh(CO)_2$ complexes. Reaction of KL^2 with the $Rh(CO)_2Cl$ dimer in THF gives conversion in less than 10 h at 25 °C to exclusively $RhL^2(CO)_2$. This compound is too poorly soluble in hexane to give an IR spectrum but is nicely soluble in benzene, giving CO stretching frequencies of 2016 and 2086 cm^{-1} for an average of 2052 cm^{-1}. This average is lower than the experimental values reported[54−60] for the bis CF_3 examples from β diketonate (2065 cm^{-1}) and monoimino ketonate (2059 cm^{-1}) analogs, showing that ligand L^2 is a moderate donor but not as electron-donating as dithiocarbamates (2038 cm^{-1}), xanthates (2025 cm^{-1}), guanidinates or amidinates (2015), trispyrazolylborates (2041 for Me_2 and 2081 for $(CF_3)_2$),[61] bisimidazole (2045 cm^{-1}), $R_2PS_2^-$ (2039 cm^{-1}), or one β diketiminate[58] (average: 2024 cm^{-1}), where the lowest frequencies are 1987 cm^{-1} and 2061 cm^{-1}. Nevertheless, many of those stronger donors would be oxidatively degraded,[26] so we feel that the pyridylpyrrolides are an appropriate compromise of electron donor power to oxidative robustness. In contrast to the above conclusions for the bis CF_3 example, the experimental CO frequencies for the bis ^{t}Bu chelate $L^0Rh(CO)_2$ of 1995 and 2066 cm^{-1}, for an average of 2027 cm^{-1}, put this ligand among the most donating of those cited above; by this criterion, the donor power of L^0 is strongly competitive with those of β-diketiminates,[57,58] which average 2021−2049 cm^{-1}. This spectroscopic contrast between L^2 and L^0 shows that varied reactivity can be anticipated and controlled by substituent character; our substituents offer a *wide* range of electronic characteristics.

The agreement with experimental results justifies confidence in the DFT CO stretching frequencies, since those faithfully exhibit the trends as CF_3 is changed to ^{t}Bu and also regarding the difference in asymmetric vs symmetric stretches within one molecule. The predictive value of DFT (e.g., toward changing metal to iridium) is thus strengthened.

Substituent Effects. It is useful to look at the substituent effect on the HOMO of pyrrole itself. Since the substituents perturb primarily the σ subspace (those symmetric to reflection in the molecule plane), will they significantly alter the energy of the HOMO, of π symmetry (orbitals antisymmetric in the molecular plane)? Figure 8 shows that the composition of the HOMO for the unsubstituted, 3,5-tBu_2, and 3,5-$(CF_3)_2$ pyrroles are very similar, but the EWG disubstitution stabilizes the HOMO by 1.4 eV (Figure 8b), while the two tBu groups raise the energy by 0.3 eV (Figure 8c). While these are in the expected direction, the different magnitudes will help identify how much impact these substituents can have in complexes of L^n. Thus, while these substitutions are essentially impacting the σ subspace of the orbitals, we see their indirect impact on the π subspace; these substituents enable a large (1.7 eV) span of redox potentials.

Comparison of Pyrrolide to Phenyl. To know the donor power of pyrrolide, the 2-pyridylphenyl ligand ppy^R, **6**, is a useful comparison standard; what is the relative donor power of pyrrolide vs phenyl? Calculations on $(L^2)Cu(CO)$, where the phenyl carries two CF_3 groups, show that its CO stretching frequency is 23 cm^{-1} lower than that of the pyrrolide analog; hence, the pyrrolide nitrogen π lone pair cannot overcome the effect of the C vs N electronegativity difference, which acts to make phenyl a better (σ) donor. Replacement of the two CF_3 groups on the phenyl of L^2 by two H lowers the CO frequency by 24 cm^{-1}; the CF_3 groups are thus confirmed to be electron-withdrawing on these rings.

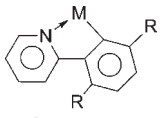

6

Frontier orbital contour diagrams reveal some remarkable differences as one moves toward the latest transition metals. In particular (Figure 9), while the HOMO of (pyridylphenyl)Rh-$(CO)_2$ is very conventionally z^2, as one generally encounters for a planar 4-coordinate d^8 complex, the situation is very different for $L^2Rh(CO)_2$, where the HOMO is dominated by a pyrrolide Cα/Cβ π orbital, with no d character. In short, the pyridylpyrrolide ligand truly brings ligand character to the forefront and is predicted to make oxidation at the metal a secondary aspect. This strong donor power of pyridylphenyl ligands apparently has its beneficial influence on the conversion of water to O_2 in a recent report of "water oxidation."[62]

Comparison to Ring Metalation Isomers. Structural isomers of pyridylpyrrolide **7** exist where the metal connection to the rings occurs at different positions (Scheme 3). These isomers are analogs of "N-confused porphyrins,"[63,64] or abnormal N-heterocyclic carbenes.[65] As pyridylpyrrolide complexes are subjected to elevated reaction temperatures, is there a possibility that these other isomers are thermodynamically preferred and thus that it would lead to pyridylpyrrolide degradation? The first isomer (**8**) involves attachment at a pyridyl vinyl carbon, leaving the nitrogen

dx.doi.org/10.1021/ic2005503 |*Inorg. Chem.* 2011, 50, 8121–8131

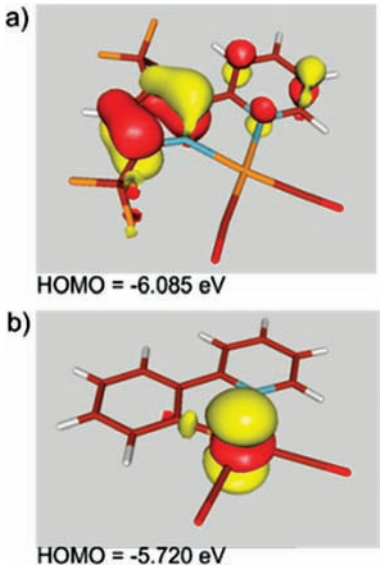

Figure 9. Isodensity diagrams of the HOMOs of (a) $L^2Rh(CO)_2$ and (b) (2-pyridylphenyl)$Rh(CO)_2$.

Scheme 3

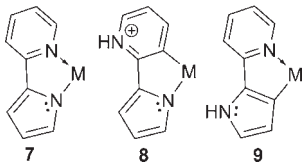

Table 3. DFT Parameters of Isomeric LM(donor)$_n$ Species[a]

	$Cu(CO)^+$			$Cu(NCMe)^+$		$Rh(CO)_2^+$	
isomer	E	ν_{CO}	∠A*−Cu−E*	E	∠A*−Cu−E*	E	ν_{CO}
7	0	2180	128°	0	125°	0	2095, 2149
8	30.5	2156	145°	32.8	157°	20.9	2079, 2133
9	26.0	2160	123°	25.9	113°	17.2	2079, 2128

[a] E in kcal/mol; ν in cm^{-1}. A* is a metal-bound atom of a monodentate ligand (NCMe or CO). E* is a metal-bound atom of a six-membered ring

protonated as a pyridinium; the ligand thus becomes a zwitterion. The alternative (**9**) is to metalate at a pyrrole ring carbon (possible when the pyrrole bears no substituents, in contrast to the pyrroles employed experimentally), thus converting the amide nitrogen to an amine; the five-membered ring thus remains a monoanion. Thus, neither of these isomers involves redox chemistry at the metal. Which isomer is more stable, and what is the relative donor power of each isomeric form? To answer the second question, we have calculated minimum energy structures for all three ligand isomers bound to the carbonyls $Cu(CO)^+$ and $Rh(CO)_2^+$. To address relative stability, and any dependence this might have on the presence/absence of a π acid ligand, we have added the pure σ monodentate example $Cu(NCMe)^+$. The results (Table 3) show that the new isomers are invariably less stable but are uniformly more donating to the metal, as reflected by the lower CO stretching frequencies. This trend holds regardless of whether the ligand is essentially a pure

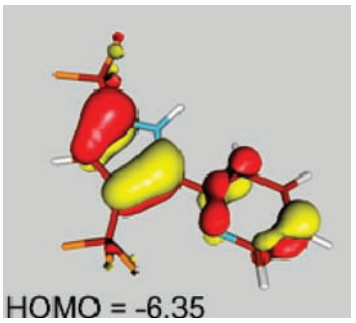

Figure 10. Isodensity diagram of the HOMO of *anti*-HL^2.

σ donor (MeCN) or a π acid (CO). Ironically, the intraligand charge separation in the zwitterionic form **8** leads to the worst energy but still has very strong donor power to the metal (as was also true for the pyridylphenyl case). A noteworthy structural feature is that the angular positioning of the CO and MeCN ligands in copper species **7**−**9** is highly variable, consistent with the high variability in the series Cu/Ag/Au already discussed above in the context of ligands L^n. The energy surface of these three-coordinate species is again shown to be highly deformable, upon small molecular changes. When the angle shown in Table 3 becomes small, the Cu/N(pyridine) distance becomes quite long.[53]

DISCUSSION

This work shows that pyridylpyrrolides can, for certain partners, establish frontier orbital character which is heavily ligand localized, and the pyrrolide participates disproportionately over the pyridyl in the HOMO. Indeed, the orbital contour diagram of the HOMO of *anti*-HL^2 (Figure 10) shows mainly pyrrole $C_\alpha-C_\beta$ character, just as is true in its copper and rhodium complexes. Moreover, the HOMO of *anti*-HL^2 is very similar to that of one frontier orbital of $Cu(L^2)_2$ (Figure 11c). The influence of the pyrrolide *substituent* was examined in terms of this orbital of all three complexes $Cu(L^n)_2$. Figure 11 shows that the orbital *composition* is nearly indistinguishable along this series, being dominated by pyrrole $C_\alpha-C_\beta$ π bonding. However, the orbital energy rises by 0.69 eV from L^2 to L^1, then another 0.59 eV from L^1 to L^0, fully consistent with the ideas of CF_3 as an electron withdrawing group and easiest oxidation with L^0. Note also that the HOMO energy of $L^2Rh(CO)_2$, of HL^2, and of the corresponding orbital of $Cu(L^2)_2$ are all −6.09 to −6.35 eV, a narrow range consistent with pyrrolide ligand localization. Finally, note that $L^nRh(CO)_2$ readily forms intact monocations under mass spectroscopic conditions, consistent with ligand-centered oxidation implicit in Figure 9a.

Are there simple trends of ligand binding of pyridyl vs pyrrolide toward metals in pyridylpyrrolide complexes? In fact, there is great variation of the comparative M/N *distances* to pyrrolide and pyridyl among available experimental determinations[23−29] of coordinated pyridylpyrrole structures, all comparing cases where the groups trans to the nitrogens are identical. There are cases where the pyrrolide is shorter, numerous examples where the two are identical, and examples, involving d^8 Au^{III} and d^6 Pt^{IV}, where the distance to the pyridyl is 0.1 shorter than to the pyrrolide. Thus, no pattern is apparent, and the pyridyl is *not* uniformly more distant. There is even one unit cell where, for two molecules in the asymmetric unit, the two show reversal of which is the shorter bond![23]

dx.doi.org/10.1021/ic2005503 |*Inorg. Chem.* 2011, 50, 8121–8131

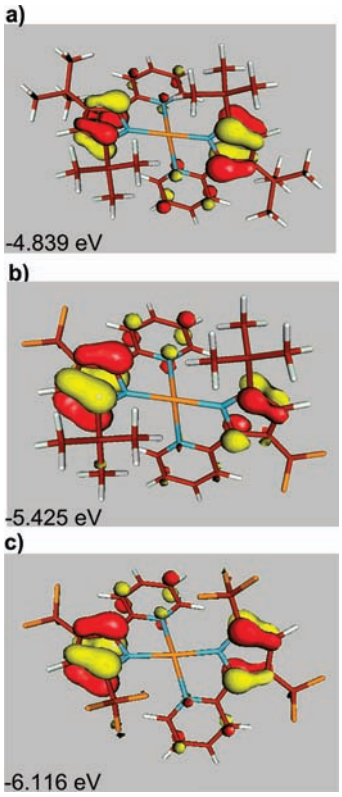

Figure 11. Isodensity diagram of one frontier orbital of (a) $Cu(L^0)_2$; (b) $Cu(L^1)_2$; (c) $Cu(L^2)_2$.

Our analysis of pyridylpyrrolide ligands shows them to have versatility beyond bipyridyls, so that pyridylpyrrolides are not simply "anionic bipy." While there is probably only modest push/pull interaction *between* the linked pyridyl π^* and the pyrrolide occupied π HOMO, the frontier orbitals of these two rings can each contribute to stabilization of oxidized (pyrrolide) or reduced (pyridyl[66−73]) metal *complexes*. The π "lone pair" of the pyrrolide nitrogen seems not to be strongly donating to these latter transition metal orbitals, judging by a spectroscopic comparison of pyridylpyrrolides to pyridylphenyl analogs; apparently that lone pair is more involved in pyrrole aromaticity. However, this analysis may also suggest that the strong reducing power[74−78] of polypyrrolide complexes of "low valent metals" may actually reside to some extent in population of the pyrrolide π^* orbitals, not only at the metal; those too may be unrecognized redox noninnocent ligand complexes. The flexibility of pyridylpyrrolides to rotation about the inter-ring bond enables this ligand to play a bridging role in $(CuL^2)_3$[44] and thus offers special opportunities in multimetal complexes; such decoupling of the two π systems when the rings are not coplanar will certainly have its impact on photophysical properties of their complexes.[24,27,29]

It must be recognized that the near absence of pyridyl orbital character in the HOMO illustrated above does not indicate that they have no significance but only that they lie lower in energy than those of pyrrolide, as forecast[79−81] by the 1 eV higher ionization potential of pyridine than of pyrrole. The pyridyl π^* orbitals participate more in the unoccupied frontier orbitals of the above complexes, indicating that the pyridylpyrrolide complexes are also subject to reduction.

One final point is the demonstrated ability[25] of this chelate to revert to monodentate binding (Scheme 4), through only the pyrrolide nitrogen, with pendant pyridyl functionality. Alternatively, when a Bronsted base is needed, the chelate can open up with only pyridyl coordinated, and the pendant pyrrolide accepts a proton. This apparently facile conversion to two different monodentate binding modes distinguishes the pyridylpyrroles from bipyridyls, a valuable difference which might be exploited productively with the former.

Scheme 4

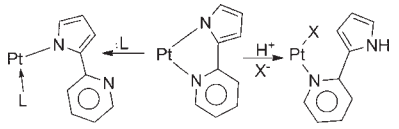

EXPERIMENTAL SECTION

General. *General Procedures.* All manipulations were carried out under an atmosphere of purified argon using standard Schlenk techniques or in a glovebox. Solvents were purchased from commercial sources, purified using the Innovative Technology SPS-400 PureSolv solvent system or by distilling from conventional drying agents, and degassed by the freeze−pump−thaw method twice prior to use. Glassware was oven-dried at 150 °C overnight. NMR spectra were recorded in C_6D_6 and CD_3CN at 25 °C on a Varian Inova-400 spectrometer (^{1}H, 400.11 MHz; ^{13}C, 100.61 MHz; ^{19}F, 376.48 MHz). Proton and carbon chemical shifts are reported in parts per million versus Me_4Si; ^{19}F NMR chemical shifts are referenced relative to external CF_3CO_2H.

Mass spectrometry analyses were performed in an Agilent 6130 MSD (Agilent Technologies, Santa Clara, CA) quadrupole mass spectrometer equipped with a Multimode (ESI and APCI) source. Ligand synthesis proceeded as described,[1,24,29] with the following improvements: For HL^0, xylene was removed in a vacuum, and the residue was washed with cold hexanes to leave white product. For HL^1, xylene was removed in a vacuum, and the residue was recrystallized from hexanes at −40 °C to give a white solid product. For HL^2, the compound has very good solubility in hexanes, and it is impossible to use crystallization. Column chromatography is thus less useful than crystallization for HL^0 and HL^1 but preferable for the large-scale preparation of L^2H.

KL^0. A total of 100 mg of L^0H (0.39 mmol) in 10 mL of THF was slowly added to the stirring mixture of 16.4 mg of KH (1.05 equiv., 0.409 mmol) in 10 mL of THF. After 30 min, gas evolution had ended and full conversion into L^0K was observed. The solution was filtered and used without further purification (removal of solvent yields solid L^0K). ^{1}H NMR of L^0K (THF d-8): 1.23 (s, 9 H, t-Bu), 1.34 (s, 9 H, t-Bu), 5.83 (s, 1 H, C−H pyrrole), 6.63 (s, 1 H, C−H Ar), 7.32 (t, J = 7.4, 1 H, C−H Ar), 7.73 (d, J = 8.0, 1 H, C−H Ar), 8.23 (d, J = 4.0, 1 H, C−H Ar).

KL^1. A total of 100 mg of L^1H (0.37 mmol) in 10 mL of THF was slowly added to a stirring mixture of 15.7 mg of KH (1.05 equiv., 0.390 mmol) in 10 mL of THF. After 30 min, gas evolution had ended and full conversion into L^1K was observed. The solution was filtered and can be used without further purification; removal of the solvent furnishes solid L^1K. ^{1}H NMR of L^1K (THF d-8): 1.27 (s, 9 H, t-Bu), 6.13 (s, 1 H, C−H pyrrole), 6.81 (m, 1 H, C−H Ar), 7.47 (t, J = 7.1, 1 H, C−H Ar), 7.58 (d, J = 8.2, 1 H, C−H Ar), 8.29 (d, J = 3.3, 1 H, C−H Ar). ^{19}F NMR (THF d-8): −51.1 (s).

KL^2. A total of 100 mg of L^2H (0.357 mmol) in 10 mL of THF was slowly added to the stirring mixture of 15.0 mg of KH (1.05 equiv., 0.374 mmol) in 10 mL of THF. After 30 min, gas evolution had ended and full conversion into L^2K was observed. The solution was filtered and dried in a vacuum to furnish solid L^2K. Crystals for structure determination were grown from a solution in Et_2O layered with pentane. ^{1}H NMR of L^2K (THF d-8): 6.63 (d, J = 0.7, 1 H, C−H pyrrole), 7.06 − 6.94 (m, 1 H, C−H Ar),

dx.doi.org/10.1021/ic2005503 |*Inorg. Chem.* 2011, 50, 8121–8131

7.64 − 7.57 (m, 1 H, C−H Ar), 7.70 − 7.64 (m, 1 H, C−H Ar), 8.42 (ddd, J = 4.8, 1.8, 1.0, 1 H, C−H Ar). ^{19}F NMR (THF d-8): −60.1 (s), −52.7 (s).

The L^2Cu(Base) for Base = CO or MeCN, preparations, and characterizations have been reported.[44] As the Bronsted acidity of HL^n diminishes, with fewer CF_3 groups and more ^{t}Bu groups, this synthetic reaction from Cu_2O in acetonitrile solvent becomes problematic and, for HL^1, appears to come to equilibrium with incomplete conversion. Attempts to shift the equilibrium using heat and reaction in the presence of molecular sieves show compete conversion for HL^1 after 5−7 days of reflux.

$L^0Rh(CO)_2$. A total of 1.8 mg of the $Rh(CO)_2Cl$ dimer (0.0093 mmol Rh) and 2.6 mg of L^0K (0.0088 mmol) were dissolved in 2 mL of THF. After 30 min at 25 °C, all volatiles were removed in a vacuum, to give an orange solid. This residue was extracted with 5 mL of benzene and dried to give 3.4 mg (88%) of the product. ^{1}H NMR (25 °C, C_6D_6): 1.45, 1.67 (both s, 9 H each, two t-Bu), 5.74−5.77 (m, 1 H, Ar−H), 6.37 (s, 1 H, Ar−H), 6.68 (ddd, J = 8.8, 7.2, 1.7 Hz, 1H, Ar−H), 7.56 (d, J = 8.7, 1H, Ar−H), 7.71 (d, J = 5.8, 1H, Ar−H). IR (KBr): 1994 and 2060. IR (C_6D_6): 1995 and 2066. MS (benzene, APCI), Exptl.: 414.1 $[M]^+$ and 415.1 $[M + H]^+$. Calcd for $C_{19}H_{23}N_2O_2Rh$, 414.1.

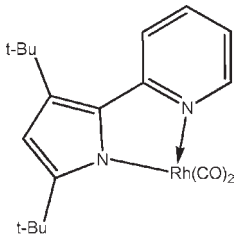

$L^2Rh(CO)_2$. A total of 1.8 mg of the $Rh(CO)_2Cl$ dimer (0.0093 mmol Rh) and 2.8 mg of L^2K (0.0088 mmol) were dissolved in 2 mL of THF. After 30 min at 25 °C, all volatiles were removed in a vacuum, to give an orange solid. This residue was extracted with 5 mL of benzene and filtered and dried to give 3.5 mg (86%) of the product. ^{1}H NMR (25 °C, C_6D_6): 5.82 (t, J = 6.0, 1 H, Ar−H), 6.67 − 6.52 (m, 1 H, Ar−H), 6.96 (s, 1 H, Ar−H), 7.35 (d, J = 4.8, 1 H, Ar−H), 7.58 (d, J = 8.4, 1 H, Ar−H). ^{19}F NMR (25 °C, C_6D_6): −56.02 (s), −57.47 (s). IR (C_6D_6): 2016 and 2086. MS (benzene, APCI), Exptl.: 438.9 $[M + H]^+$. Calcd for $C_{13}H_5F_6N_2O_2Rh$, 437.9.

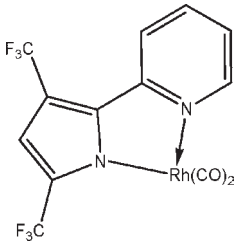

■ ASSOCIATED CONTENT

Ⓢ Supporting Information. Computational results and NMR spectra. This material is available free of charge via the Internet at http://pubs.acs.org.

■ AUTHOR INFORMATION

Corresponding Author
*E-mail: caulton@indiana.edu.

■ ACKNOWLEDGMENT

This work was supported by a grant to K.G.C. (CHE-0749386) by the National Science Foundation. D.L.L. thanks the National Science Foundation through the Project CHE-0749530. A.R.H. thanks the Department of Chemistry and Biochemistry, The University of Arizona, for support of the Molecular Photoelectron Spectroscopy Facility.

■ REFERENCES

(1) Klappa, J. J.; Rich, A. E.; McNeill, K. *Org. Lett.* **2002**, *4*, 435.
(2) Carabineiro, S. A.; Silva, L. C.; Gomes, P. T.; Pereira, L. C. J.; Veiros, L. F.; Pascu, S. I.; Duarte, M. T.; Namorado, S.; Henriques, R. T. *Inorg. Chem.* **2007**, *46*, 6880.
(3) Carabineiro, S. A.; Bellabarba, R. M.; Gomes, P. T.; Pascu, S. I.; Veiros, L. F.; Freire, C.; Pereira, L. C. J.; Henriques, R. T.; Oliveira, M. C.; Warren, J. E. *Inorg. Chem.* **2008**, *47*, 8896.
(4) Mashima, K.; Tsurugi, H. *J. Organomet. Chem.* **2005**, *690*, 4414.
(5) Hao, J.; Song, H.; Cui, C. *Organometallics* **2009**, *28*, 3100.
(6) Cohen, S. M.; Halper, S. R. *Inorg. Chim. Acta* **2002**, *341*, 12.
(7) Hill, C. L.; Williamson, M. M. *J. Chem. Soc., Chem. Commun.* **1985**, 1228.
(8) King, E. R.; Betley, T. A. *Inorg. Chem.* **2009**, *48*, 2361.
(9) Murakami, Y.; Matsuda, Y.; Sakata, K. *Inorg. Chem.* **1971**, *10*, 1728.
(10) Murakami, Y.; Matsuda, Y.; Sakata, K. *Inorg. Chem.* **1971**, *10*, 1734.
(11) Murakami, Y.; Sakata, K. *Bull. Chem. Soc. Jpn.* **1974**, *47*, 3025.
(12) Odom, A. L. *Dalton Trans.* **2005**, 225.
(13) Swartz, D. L., II; Spencer, L. P.; Scott, B. L.; Odom, A. L.; Boncella, J. M. *Dalton Trans.* **2010**, *39*, 6841.
(14) Tang, X.; Sun, W.-H.; Gao, T.; Hou, J.; Chen, J.; Chen, W. *J. Organomet. Chem.* **2005**, *690*, 1570.
(15) Perez-Puente, P.; de Jesus, E.; Flores, J. C.; Gomez-Sal, P. *J. Organomet. Chem.* **2008**, *693*, 3902.
(16) Benito, J. M.; de Jesus, E.; de la Mata, F. J.; Flores, J. C.; Gomez, R.; Gomez-Sal, P. *Organometallics* **2006**, *25*, 3876.
(17) Dawson, D. M.; Walker, D. A.; Thornton-Pett, M.; Bochmann, M. *Dalton* **2000**, 459.
(18) Sazama, G. T.; Betley, T. A. *Inorg. Chem.* **2010**, *49*, 2512.
(19) King, E. R.; Betley, T. A. *J. Am. Chem. Soc.* **2009**, *131*, 14374.
(20) Chi, Y.; Chou, P.-T. *Chem. Soc. Rev.* **2010**, *39*, 638.
(21) Chi, Y.; Chou, P.-T. *Chem. Soc. Rev.* **2007**, *36*, 1421.
(22) Caris, R.; Peoples, B. C.; Valderrama, M.; Wu, G.; Rojas, R. *J. Organomet. Chem.* **2009**, *694*, 1795.
(23) McBee, J. L.; Tilley, T. D. *Organometallics* **2009**, *28*, 3947.
(24) Pucci, D.; Aiello, I.; Aprea, A.; Bellusci, A.; Crispini, A.; Ghedini, M. *Chem. Commun.* **2009**, 1550.
(25) Chen, J.-L.; Lin, C.-H.; Chen, J.-H.; Chi, Y.; Chiu, Y.-C.; Chou, P.-T.; Lai, C.-H.; Lee, G.-H.; Carty, A. J. *Inorg. Chem.* **2008**, *47*, 5154.
(26) Luedtke, A. T.; Goldberg, K. I. *Inorg. Chem.* **2007**, *46*, 8496.
(27) Shih, P.-I.; Chien, C.-H.; Chuang, C.-Y.; Shu, C.-F.; Yang, C.-H.; Chen, J.-H.; Chi, Y. *J. Mater. Chem.* **2007**, *17*, 1692.
(28) Schouteeten, S.; Allen, O. R.; Haley, A. D.; Ong, G. L.; Jones, G. D.; Vicic, D. A. *J. Organomet. Chem.* **2006**, *691*, 4975.
(29) Klappa, J. J.; Geers, S. A.; Schmidtke, S. J.; MacManus-Spencer, L. A.; McNeill, K. *Dalton Trans.* **2004**, 883.
(30) Jones, C.; Rose, R. P. *New J. Chem.* **2007**, *31*, 1484.
(31) Hansch, C.; Gao, H. *Chem. Rev.* **1997**, *97*, 2995.
(32) Jones, R. A.; Spotswood, T. M.; Cheuychit, P. *Tetrahedron* **1967**, *23*, 4469.
(33) Cherkasov, V. K.; Abakumov, G. A.; Grunova, E. V.; Poddel'sky, A. I.; Fukin, G. K.; Baranov, E. V.; Kurskii, Y. V.; Abakumova, L. G. *Chem.—Eur. J.* **2006**, *12*, 3916.
(34) Lippert, C. A.; Soper, J. D. *Inorg. Chem.* **2010**, *49*, 3682.
(35) Lippert, C. A.; Arnstein, S. A.; Sherrill, C. D.; Soper, J. D. *J. Am. Chem. Soc.* **2010**, *132*, 3879.
(36) Blackmore, K. J.; Sly, M. B.; Haneline, M. R.; Ziller, J. W.; Heyduk, A. F. *Inorg. Chem.* **2008**, *47*, 10522.
(37) Ketterer, N. A.; Fan, H.; Blackmore, K. J.; Yang, X.; Ziller, J. W.; Baik, M.-H.; Heyduk, A. F. *J. Am. Chem. Soc.* **2008**, *130*, 4364.

(38) Haneline, M. R.; Heyduk, A. F. *J. Am. Chem. Soc.* **2006**, *128*, 8410.
(39) Mukherjee, C.; Weyhermueller, T.; Bothe, E.; Chaudhuri, P. *Inorg. Chem.* **2008**, *47*, 2740.
(40) Fedushkin, I. L.; Maslova, O. V.; Hummert, M.; Schumann, H. *Inorg. Chem.* **2010**, *49*, 2901.
(41) Fedushkin, I. L.; Makarov, V. M.; Sokolov, V. G.; Fukin, G. K. *Dalton Trans.* **2009**, 8047.
(42) Fedushkin, I. L.; Skatova, A. A.; Lukoyanov, A. N.; Khvoinova, N. M.; Piskunov, A. V.; Nikipelov, A. S.; Fukin, G. K.; Lysenko, K. A.; Irran, E.; Schumann, H. *Dalton Trans.* **2009**, 4689.
(43) Franklin, J. L. *J. Am. Chem. Soc.* **1950**, *72*, 4278.
(44) Andino, J. G.; Flores, J. A.; Karty, J. A.; Massa, J. P.; Park, H.; Tsvetkov, N. P.; Wolfe, R. J.; Caulton, K. G. *Inorg. Chem.* **2010**, *49*, 7626.
(45) Wang, H.; Zeng, Y.; Ma Jin, S.; Fu, H.; Yao, J.; Mikhaleva, A. I.; Trofimov, B. A. *Chem. Commun.* **2009**, 5457.
(46) Derrick, P. J.; Asbrink, L.; Edqvist, O.; Jonsson, B. O.; Lindholm, E. *Int. J. Mass Spectrom. Ion Phys.* **1971**, *6*, 191.
(47) Derrick, P. J.; Asbrink, L.; Edqvist, O.; Lindholm, E. *Spectrochim. Acta, Part A* **1971**, *27*, 2525.
(48) Ramsey, B. G.; Walker, F. A. *J. Am. Chem. Soc.* **1974**, *96*, 3314.
(49) Heilbronner, E.; Hornung, V.; Pinkerton, F. H.; Thames, S. F. *Helv. Chim. Acta* **1972**, *55*, 289.
(50) Holland, P. L.; Rodgers, K. R.; Tolman, W. B. *Angew. Chem., Int. Ed.* **1999**, *38*, 1139.
(51) Dias, H. V. R.; Lovely, C. J. *Chem. Rev.* **2008**, *108*, 3223.
(52) Lupinetti, A. J.; Strauss, S. H.; Frenking, G. *Prog. Inorg. Chem.* **2001**, *49*, 1.
(53) See the Supporting Information.
(54) Heras, J. V.; Pinilla, E.; Ovejero, P. *J. Organomet. Chem.* **1987**, *332*, 213.
(55) Faraone, F. *J. Chem. Soc., Dalton Trans.* **1975**, 541.
(56) Varshavsky, Y. S.; Galding, M. R.; Cherkasova, T. G.; Smirnov, S. N.; Khrustalev, V. N. *J. Organomet. Chem.* **2007**, *692*, 5788.
(57) Shaffer, D. W.; Ryken, S. A.; Zarkesh, R. A.; Heyduk, A. F. *Inorg. Chem.* **2010**, ASAP.
(58) Fandos, R.; Walter, M. D.; Kazhdan, D.; Andersen, R. A. *Organometallics* **2006**, *25*, 3678.
(59) Edelmann, F. T. *Adv. Organomet. Chem.* **2008**, *57*, 183.
(60) Hagadorn, J. R.; Arnold, J. *J. Organomet. Chem.* **2001**, *637–639*, 521.
(61) Moszner, M.; Wolowiec, S.; Trosch, A.; Vahrenkamp, H. *J. Organomet. Chem.* **2000**, *595*, 178.
(62) Hull, J. F.; Balcells, D.; Blakemore, J. D.; Incarvito, C. D.; Eisenstein, O.; Brudvig, G. W.; Crabtree, R. H. *J. Am. Chem. Soc.* **2009**, *131*, 8730.
(63) Srinivasan, A.; Toganoh, M.; Niino, T.; Osuka, A.; Furuta, H. *Inorg. Chem.* **2008**, *47*, 11305.
(64) Won, D.-H.; Toganoh, M.; Uno, H.; Furuta, H. *Dalton Trans.* **2009**, 6151.
(65) Appelhans, L. N.; Incarvito, C. D.; Crabtree, R. H. *J. Organomet. Chem.* **2008**, *693*, 2761.
(66) Kraft, S. J.; Fanwick, P. E.; Bart, S. C. *Inorg. Chem.* **2010**, *49*, 1103.
(67) Echegoyen, L.; Perez-Cordero, E.; Regnouf de Vains, J. B.; Roth, C.; Lehn, J. M. *Inorg. Chem.* **1993**, *32*, 572.
(68) Perez-Cordero, E.; Buigas, R.; Brady, N.; Echegoyen, L.; Arana, C.; Lehn, J. M. *Helv. Chim. Acta* **1994**, *77*, 1222.
(69) Wagner, M. J.; Dye, J. L.; Perez-Cordero, E.; Buigas, R.; Echegoyen, L. *J. Am. Chem. Soc.* **1995**, *117*, 1318.
(70) Perez-Cordero, E. E.; Campana, C.; Echegoyen, L. *Angew. Chem., Int. Ed.* **1997**, *36*, 137.
(71) Broudy, P. M.; Berry, A. D.; Wayland, B. B.; MacDiarmid, A. G. *J. Am. Chem. Soc.* **1972**, *94*, 7577.
(72) Chisholm, M. H.; Huffman, J. C.; Rothwell, I. P.; Bradley, P. G.; Kress, N.; Woodruff, W. H. *J. Am. Chem. Soc.* **1981**, *103*, 4945.
(73) Chisholm, M. H.; Kober, E. M.; Ironmonger, D. J.; Thornton, P. *Polyhedron* **1985**, *4*, 1869.
(74) Korobkov, I.; Vidjayacoumar, B.; Gorelsky, S. I.; Billone, P.; Gambarotta, S. *Organometallics* **2010**, *29*, 692.
(75) Korobkov, I.; Gambarotta, S.; Yap, G. P. A. *Organometallics* **2001**, *20*, 2552.
(76) Yunlu, K.; Basolo, F.; Rheingold, A. L. *J. Organomet. Chem.* **1987**, *330*, 221.
(77) Solari, E.; Crescenzi, R.; Jacoby, D.; Floriani, C.; Chiesi-Villa, A.; Rizzoli, C. *Organometallics* **1996**, *15*, 2685.
(78) Franceschi, F.; Guillemot, G.; Solari, E.; Floriani, C.; Re, N.; Birkedal, H.; Pattison, P. *Chemistry* **2001**, *7*, 1468.
(79) Williamson, A. D.; Compton, R. N.; Eland, J. H. D. *J. Chem. Phys.* **1979**, *70*, 590.
(80) Cooper, C. D.; Williamson, A. D.; Miller, J. C.; Compton, R. N. *J. Chem. Phys.* **1980**, *73*, 1527.
(81) Nakatsuji, H.; Kitao, O.; Yonezawa, T. *J. Chem. Phys.* **1985**, *83*, 723.